Magnetic polarons in the Kondo lattice

R. Eder [1] and P. Wróbel [2]

[1] *Karlsruhe Institute of Technology, Institute for Quantum Materials and Technologies, 76021 Karlsruhe, Germany*

[2] *Institute of Low Temperature and Structure Research, ul. Okólna 2, 50-422 Wrocław, Poland*

(Received 9 April 2024; revised 31 May 2024; accepted 21 June 2024; published 3 July 2024)

We investigate the formation of magnetic polarons in the Kondo lattice model. Calculations are done in the framework of the bond particle formalism. We show that the quasiparticles correspond to spin polarons with a **k**-dependent spatial extent. Polaron formation leads to a significant enhancement of the effective mass in the *heavy* parts of the band structure.

DOI: 10.1103/PhysRevB.110.035112

I. INTRODUCTION

Heavy fermion compounds are a much studied field of solid state physics. These materials show a number of remarkable phenomena which are widely believed to be caused by the strong Coulomb repulsion between the electrons in the $4f$ shells of rare earth elements or the $5f$ shell of actinides. In particular, they show a crossover from a high temperature state, where a lattice of localized f electrons coexists with weakly or moderately correlated conduction electron bands, to an exotic Fermi liquid with high effective masses at low temperature, where the f electrons now contribute to the Fermi-surface volume [1,2]. Heavy fermion compounds can be described by the Kondo-lattice model (KLM) which is derived from the more realistic periodic Anderson model (PAM) by means of the Schrieffer-Wolff transformation [3]. In the simplest case of no orbital degeneracy each unit cell n contains one f orbital and one conduction band orbital, and denoting the creation operators for electrons in these orbitals by $f^\dagger_{n,\sigma}$ and $c^\dagger_{n,\sigma}$ the Kondo lattice Hamiltonian is $H_{\rm KLM} = H_t + H_J$ with

$$H_t = \sum_{m,n} \sum_{\sigma} t_{m,n}\, c^\dagger_{m,\sigma} c_{n,\sigma}, \quad H_J = J \sum_n \boldsymbol{S}_{n,c} \cdot \boldsymbol{S}_{n,f},$$

$$\boldsymbol{S}_{n,c} = \frac{1}{2} \sum_{\sigma,\sigma'} c^\dagger_{n,\sigma}\, \boldsymbol{\tau}_{\sigma,\sigma'}\, c_{n,\sigma'}. \tag{1}$$

Here $\boldsymbol{\tau}$ denotes the vector of Pauli matrices and an analogous definition holds for $\boldsymbol{S}_{n,f}$. Inherent to the model is the constraint $\sum_\sigma f^\dagger_{n,\sigma} f_{n,\sigma} = 1$ which must hold separately for each n and reflects the strong-coupling nature of the KLM. In the following we consider a two-dimensional square lattice with N unit cells and N conduction electrons, a case frequently referred to as the Kondo insulator. Throughout we assume that $t_{m,n} = -t$ for nearest neighbors m and n and zero otherwise and we choose t as the unit of energy. The generalization to longer range hopping integrals is straightforward.

The impurity versions of the Kondo and Anderson model are well understood. In addition to various approximate calculations [4–12] they can be solved exactly by renormalization group [13] and Bethe ansatz [14]. All calculations agree in that the ground state is a singlet formed from the f electron on the impurity and an extended but localized state formed from conduction band states, whereby for weak coupling ($J \ll t$) the binding energy—the so-called Kondo temperature—is $k_B T_K \propto W e^{-1/\rho J}$ (W and ρ are bandwidth and density of states of the conduction band).

The lattice versions of the model are less well understood. Approximate results have been obtained by mean-field approximation both to the KLM [15–26] and the PAM [27,28] and in addition a variety of numerical methods have been applied to these models [29–52]. The resulting band structure is consistent with a simple hybridization picture: a dispersionless effective f band close to the Fermi energy of the decoupled conduction electron system hybridizes with the conduction electron band via some effective hybridization matrix element. Mean-field theories predict the strength of the hybridization matrix element to be $\propto k_B T_K$ at weak coupling, the inverse of which accordingly sets the scale for the band mass of the effective f band. This results in a Fermi surface with a volume corresponding to itinerant f electrons [53] and the *heavy bands* characteristic of heavy fermion compounds. These features are qualitatively reproduced by numerical studies but it should be noted that these usually have problems accessing the limit of small J/t and thus do not reproduce the Kondo scale $k_B T_K$ for the heavy bands.

As pointed out by Nozières [54], it is not immediately obvious why the Kondo scale $k_B T_K$ for the impurity models should play a role in the lattice case and determine, e.g., the width of the heavy bands. Namely in the impurity models only a very small fraction $\propto e^{-1/\rho J}$ of the conduction electrons takes part in the formation of the Kondo screening cloud. It is unclear how this small fraction of conduction electrons can simultaneously screen an entire lattice of magnetic impurities—the famous Nozières exhaustion problem [54]. This raises the question of whether the large band mass in heavy fermion systems is really related to the impurity Kondo effect. In the following we want to discuss a mechanism which can enhance the effective masses in the heavy bands considerably, namely the formation of magnetic polarons.

II. BOND PARTICLE FORMULATION

Bond particle theory was proposed originally by Sachdev and Bhatt [55] and was used subsequently to study spin

systems and applied to spin ladders [56], bilayers [57,58], intrinsically dimerized spin systems [59,60], and the *Kondo necklace* [61]. It was also applied to the PAM [62] and antiferromagnetic ordering in the planar KLM [63,64]. In bond particle theory the eigenstates of the single-cell Hamiltonian $h_n = J\, \boldsymbol{S}_{n,f} \cdot \boldsymbol{S}_{n,c}$ are represented as bosons (for eigenstates with even electron number) or fermions (for odd electron number). More precisely, one identifies

$$\frac{1}{\sqrt{2}} \sum_{\sigma,\sigma'} c^\dagger_{n,\sigma}\, (i\tau_y)_{\sigma,\sigma'}\, f^\dagger_{n,\sigma'}|0\rangle \to s^\dagger_n|0\rangle, \quad \frac{1}{\sqrt{2}} \sum_{\sigma,\sigma'} c^\dagger_{n,\sigma}\, (\boldsymbol{\tau} i\tau_y)_{\sigma,\sigma'}\, f^\dagger_{n,\sigma'}|0\rangle \to \boldsymbol{t}^\dagger_n|0\rangle,$$
$$f^\dagger_{n,\sigma}|0\rangle \to a^\dagger_{n,\sigma}|0\rangle, \quad c^\dagger_{n,\uparrow} c^\dagger_{n,\downarrow} f^\dagger_{n,\sigma}|0\rangle \to b^\dagger_{n,\sigma}|0\rangle. \tag{2}$$

The physical sector of the bond particle Hilbert space is defined by the constraint

$$s^\dagger_n s_n + \sum_\sigma (a^\dagger_{n,\sigma} a_{n,\sigma} + b^\dagger_{n,\sigma} b_{n,\sigma}) + \boldsymbol{t}^\dagger_n \cdot \boldsymbol{t}_n = 1, \tag{3}$$

because only if this is obeyed in every cell n the bond particle state can be uniquely translated back to a state of the original KLM.

We identify the eigenvalue of h_n as the energy of the respective bond particle; i.e., the singlet boson created by $s^\dagger_n$ has energy $-3J/4$, the three triplet bosons $\boldsymbol{t}^\dagger_n$ have energy $J/4$, whereas the holelike fermion $a^\dagger_{n,\sigma}$ and the electronlike fermion $b^\dagger_{n,\sigma}$ have energy zero. Accordingly, using (3), the exchange term can be written as

$$H_J = \sum_n \left\{ \frac{3J}{4} \sum_\sigma (b^\dagger_{n,\sigma} b_{n,\sigma} + a^\dagger_{n,\sigma} a_{n,\sigma}) + J\, \boldsymbol{t}^\dagger_n \cdot \boldsymbol{t}_n \right\} - \frac{3NJ}{4}. \tag{4}$$

From now on we take a fermion operator with omitted spin index to denote a two-component spinor, e.g.,

$$c_n = \begin{pmatrix} c_{n,\uparrow} \\ c_{n,\downarrow} \end{pmatrix}. \tag{5}$$

The electron annihilation operator then takes the form

$$c_n = \frac{1}{\sqrt{2}}\ :[(s_n + \boldsymbol{t}_n \cdot \boldsymbol{\tau})\, i\tau_y a^\dagger_n - (s^\dagger_n - \boldsymbol{t}^\dagger_n \cdot \boldsymbol{\tau})\, b_n]: \tag{6}$$

where $:\cdots:$ denotes normal ordering. Inserting this into H_t in (1) one finds [65] $H_t = H_1 + H_2 + H_3 + H_4$ with

$$H_1 = \sum_{m,n} \frac{t_{m,n}}{2} \sum_\sigma (b^\dagger_{m,\sigma} b_{n,\sigma} - a^\dagger_{m,\sigma} a_{n,\sigma})\, s^\dagger_n\, s_m - \sum_{m,n} \frac{t_{m,n}}{2} [(b^\dagger_{m,\uparrow} a^\dagger_{n,\downarrow} - b^\dagger_{m,\downarrow} a^\dagger_{n,\uparrow})\, s_m\, s_n + \text{H.c.}],$$
$$H_2 = \sum_{m,n} \frac{t_{m,n}}{2} \sum_\sigma (b^\dagger_{m,\sigma} b_{n,\sigma} - a^\dagger_{m,\sigma} a_{n,\sigma})\, \boldsymbol{t}^\dagger_n \cdot \boldsymbol{t}_m + \sum_{m,n} \frac{t_{m,n}}{2} [(b^\dagger_{m,\uparrow} a^\dagger_{n,\downarrow} - b^\dagger_{m,\downarrow} a^\dagger_{n,\uparrow}) \boldsymbol{t}_m \cdot \boldsymbol{t}_n + \text{H.c.}],$$
$$H_3 = -\sum_{m,n} \frac{t_{m,n}}{2} \{[\boldsymbol{\pi}^\dagger_{m,n} \cdot (s_m\, \boldsymbol{t}_n - \boldsymbol{t}_m\, s_n) + \text{H.c.}] + (\boldsymbol{b}_{m,n} - \boldsymbol{a}_{m,n}) \cdot (\boldsymbol{t}^\dagger_n\, s_m + s^\dagger_n\, \boldsymbol{t}_m)\},$$
$$H_4 = \sum_{m,n} \frac{t_{m,n}}{2} \{[i\boldsymbol{\pi}^\dagger_{m,n} \cdot (\boldsymbol{t}_m \times \boldsymbol{t}_n) + \text{H.c.}] - i\, (\boldsymbol{b}_{m,n} - \boldsymbol{a}_{m,n}) \cdot (\boldsymbol{t}^\dagger_n \times \boldsymbol{t}_m)\}. \tag{7}$$

The vectors $\boldsymbol{b}_{m,n}$ and $\boldsymbol{b}_{m,n}$ in H_3 and H_4 are defined as

$$\boldsymbol{b}_{m,n} = \sum_{\sigma,\sigma'} b^\dagger_{m,\sigma}\, \boldsymbol{\tau}_{\sigma,\sigma'}\, b_{n,\sigma'}, \tag{8}$$

and analogously for $\boldsymbol{a}_{m,n}$, whereas the vector $\boldsymbol{\pi}^\dagger_{m,n}$ is defined as

$$\boldsymbol{\pi}^\dagger_{m,n} = \sum_{\sigma,\sigma'} b^\dagger_{m,\sigma}\, (\boldsymbol{\tau}\, i\tau_y)_{\sigma,\sigma'}\, a^\dagger_{n,\sigma'}.$$

Strictly speaking the individual terms in H_t have to be *sitewise normal ordered*, e.g., $b^\dagger_{m,\sigma} b_{n,\sigma} t^\dagger_{n,\alpha} t_{m,\alpha} \to b^\dagger_{m,\sigma} t_{m,\alpha} t^\dagger_{n,\alpha} b_{n,\sigma}$, but since this normal ordering always involves commutation of a fermion and a boson neither nonvanishing commutators nor Fermi signs will arise.

The quartic terms H_1 and H_2 can be treated in mean-field approximation, which has been carried out in Ref. [65]. The term H_4 also would lend itself to mean-field factorization, but this would result in exotic magnetic order parameters formed from the triplets such as $\langle \boldsymbol{t}^\dagger_n \times \boldsymbol{t}_m \rangle$ or $\langle \boldsymbol{t}^\dagger_n \times \boldsymbol{t}^\dagger_m \rangle$ which we do not consider here. Instead, in the following we focus on the term H_3. In a mean-field treatment this would requite a condensation of triplets, i.e., $\langle \boldsymbol{t}^\dagger_n \rangle \neq 0$, which is equivalent to magnetic ordering. This has been considered elsewhere [63,66,67] and here we focus instead on another aspect of this term, namely the formation of *magnetic polarons*.

III. PROPAGATION OF A SINGLE FERMION

As a preliminary study we consider the motion of a single $b^\dagger$-like fermion added to the Kondo insulator. Thereby

we will closely follow the well-known treatment of a single hole in an antiferromagnet as described by the $t-J$ model. This has been studied in a variety of ways [68–72] and the solution is quite reliable in that it agrees well with numerical studies [73–75] and also with angle resolved photoemission experiments on cuprate materials [76].

We collect the terms which describe just a single $b^\dagger$-like fermion from H_J, the first term of H_1, and the second term in H_3:

$$\begin{aligned} H_{b,0} &= \sum_n \left(\frac{3J}{4} \sum_\sigma b^\dagger_{n,\sigma} b_{n,\sigma} + J\, \boldsymbol{t}^\dagger_n \cdot \boldsymbol{t}_n \right), \\ H_{b,1} &= \sum_{m,n} \frac{t_{m,n}}{2} \sum_\sigma b^\dagger_{m,\sigma} b_{n,\sigma}\, s^\dagger_n\, s_m, \\ H_{b,2} &= -\sum_{m,n} \frac{t_{m,n}}{2}\, T_{m,n}, \\ T_{m,n} &= \sum_{\sigma,\sigma'} b^\dagger_{m,\sigma}\, \boldsymbol{\tau}_{\sigma,\sigma'}\, b_{n,\sigma'} \cdot (\boldsymbol{t}^\dagger_n\, s_m + s^\dagger_n\, \boldsymbol{t}_m). \end{aligned} \tag{9}$$

$H_{b,0}$ describes the exchange energy of the various particles, $H_{b,1}$ the direct hopping of the $b^\dagger$ fermion, and $H_{b,2}$ hopping of the $b^\dagger$ fermion with a triplet being *radiated off* or *absorbed*. We start out with a normalized state with a single $b^\dagger$-like particle at site n_0:

$$|n_0\rangle = b^\dagger_{n_0,\uparrow} \prod_{n\neq n_0} s^\dagger_n |0\rangle. \tag{10}$$

We arbitrarily assign an $\uparrow$ spin to the fermion, and the following development can be carried out *mutatis mutandis* for a $\downarrow$ spin. Let n_1 be a nearest neighbor of n_0, then

$$T_{n_1,n_0}|n_0\rangle = [b^\dagger_{n_1,\downarrow}(t^\dagger_{n_0,x} + it^\dagger_{n_0,y}) + b^\dagger_{n_1,\uparrow} t^\dagger_{n_0,z}] \prod_{n\neq n_0,n_1} s^\dagger_n |0\rangle. \tag{11}$$

The right-hand side is the sum of three orthonormal states with coefficients that have unit modulus, the norm of which is 3. We can continue like this and consider a sequence of sites $n_0, n_1, n_2, \ldots, n_\nu$ such that n_{i+1} is a nearest neighbor of n_i and all $\nu+1$ sites are pairwise unequal. In other words the $\nu+1$ sites $n_0, n_1, n_2, \ldots, n_\nu$ form a non-self-intersecting path of nearest neighbors which connects n_0 and n_ν. Then consider

$$\prod_{i=0}^{\nu-1} T_{n_{i+1},n_i}\, |n_0\rangle. \tag{12}$$

This is the sum of $N_\nu = 3^\nu$ orthonormal states each of which has a total of $\nu \mathbf{t}^\dagger$ bosons at the sites $n_0, n_1, n_2, \ldots, n_{\nu-1}$ and a $b^\dagger$ fermion at site n_ν. All N_ν states have coefficients with modulus 1. Accordingly, the state

$$|n_0, n_1, n_2, \ldots, n_\nu\rangle = \frac{1}{\sqrt{N_\nu}} \prod_{i=0}^{\nu-1} T_{n_{i+1},n_i}\, |n_0\rangle \tag{13}$$

has norm 1 and we call this a *string state*. It corresponds to the $b^\dagger$ fermion hopping along the path $n_0, n_1, n_2, \ldots, n_\nu$ thereby radiating off a triplet in each step and the spins of the triplets and the $b^\dagger$ fermion are always coupled to a spin of $S = 1/2$.

Obviously

$$\langle n_0, \ldots, n_\nu | H_{b,0} | n_0, \ldots, n_\nu \rangle = \nu J + \frac{3J}{4}. \tag{14}$$

Next, consider the matrix element of $H_{b,2}$ between two successive string states $|n_0, n_1, n_2, \ldots, n_\nu\rangle$ and $|n_0, n_1, n_2, \ldots, n_\nu, n_{\nu+1}\rangle$:

$$\begin{aligned} \langle n_0, \ldots, n_\nu, n_{\nu+1} | H_{b,2} | n_0, \ldots, n_\nu \rangle &= -\frac{t_{n_{\nu+1},n_\nu}}{2} \frac{N_{\nu+1}}{\sqrt{N_\nu N_{\nu+1}}} \\ &= \frac{\sqrt{3}\, t}{2}. \end{aligned} \tag{15}$$

We call $\tilde{t} = \sqrt{3}\, t/2$. So far we have considered only one path $n_0, n_1, n_2, \ldots, n_\nu$, but clearly there are many of them. More precisely, if we denote the number of nearest neighbors of a given site by z, the number of different paths $n_0, n_1, n_2, \ldots, n_\nu$ is approximately

$$l_\nu = \begin{cases} 1 & \nu = 0, \\ z & \nu = 1, \\ z(z-1)^{\nu-1} & \nu > 1. \end{cases} \tag{16}$$

This is exact for $\nu \leqslant 3$ but then the first self-intersecting paths become possible and the exact l_ν is less than this. However, we adopt the Bethe-lattice approximation for simplicity and assume this to hold true for any ν. Then, we make the following ansatz for a magnetic polaron centered on the site n_0:

$$|\phi_{n_0}\rangle = \sum_{\nu=0}^{\infty} \alpha_\nu \sum_{n_1,n_2,\ldots,n_\nu}{}' |n_0, n_1, n_2, \ldots, n_\nu\rangle. \tag{17}$$

The prime on the sum indicates that we are summing over all sets of sites $\{n_0, n_1, n_2, \ldots, n_\nu\}$ which form a non-self-intersecting path of nearest neighbors and the α_ν are real variational parameters. This may be thought of as a state where the fermion starts out from site n_0 and hops along a given path, thereby radiating off a triplet at each step, but since the energy increases linearly with the number of triplets—see Eq. (14)—the fermion is eventually forced to return to n_0, from which it starts anew along a different path and so on. We assume that all strings of a given length ν have the same coefficient α_ν irrespective of their geometry, which is plausible because all strings of the same length have the same energy. The norm of a state of the type (17) is

$$\langle \phi_n | \phi_n \rangle = \sum_{\nu=0}^{\infty} l_\nu\, \alpha_\nu^2 = \sum_{\nu=0}^{\infty} \beta_\nu^2, \tag{18}$$

where we have introduced $\beta_\nu = \sqrt{l_\nu}\, \alpha_\nu$. The expectation value of the Hamiltonian is

$$\begin{aligned} \langle \phi_n | H_b | \phi_n \rangle &= \sum_{\nu=0}^{\infty} \left[2\tilde{t}\, l_{\nu+1}\, \alpha_{\nu+1}\alpha_\nu + l_\nu\, \epsilon_\nu\, \alpha_\nu^2 \right] \\ &= \sum_{\nu=0}^{\infty} \left[2\tilde{t}\, f_\nu\, \beta_{\nu+1}\beta_\nu + \epsilon_\nu\, \beta_\nu^2 \right], \end{aligned} \tag{19}$$

where $f_0 = \sqrt{z}$ and $f_\nu = \sqrt{z-1}$ otherwise. We may now introduce a cutoff $\nu_{\max}$ for the length of the string and perform

the variational procedure with respect to β_ν. This results in the Hermitian eigenvalue problem

$$\epsilon_0\beta_0 + \tilde{t} f_0 \beta_1 = E\ \beta_0,$$
$$\tilde{t} f_{\nu-1}\beta_{\nu-1} + \epsilon_\nu \beta_\nu + \tilde{t} f_\nu \beta_{\nu+1} = E\ \beta_\nu, \qquad (20)$$

where the second line holds for $\nu \geqslant 1$. We denote the ith eigenvalue and eigenfunction by E_i and $|\phi_{n,i}\rangle$, and the coefficients of the latter are denoted by $\beta_{\nu,i}$.

So far we have considered a self-trapped state centered on a given site n_0. In addition to $H_{b,2}$ which describes hopping combined with emission/absorption of a triplet, we also have the term $H_{b,1}$ which describes simple hopping of the fermion. $H_{b,1}$ could transport the fermion at the end of a string state $|n_0, n_1, n_2, \ldots, n_\nu\rangle$ to some site $m \neq n_i$ for any i. This would mean that the string of triplets is detached from the hole or, put another way, the fermion radiates off the entire string of triplets. Such a process cannot contribute to the *coherent* motion of the magnetic polaron. The only way to translate the polaron without *leaving a trace* is to act with $H_{b,2}$ on the *string of length zero* $|n_0\rangle$. Since the coefficient of this state in $|\phi_{n,i}\rangle$ is $\beta_{0,i}$ the matrix element of $H_{b,1}$ between two magnetic polaron states at the sites $m \neq n$ is

$$\langle\phi_{m,i}|H|\phi_{n,j}\rangle = \frac{t_{m,n}}{2}\ \beta_{0,i}\ \beta_{0,j}. \qquad (21)$$

Moreover, any two self-trapped states centered on different sites $m \neq n$ are orthogonal:

$$\langle\phi_{m,i}|H|\phi_{n,j}\rangle = \delta_{m,n}\ \delta_{i,j}. \qquad (22)$$

Accordingly we construct orthonormal Bloch states

$$|\phi_{\mathbf{k},i}\rangle = \frac{1}{\sqrt{N}} \sum_n e^{i\mathbf{k}\cdot\mathbf{R}_n}\ |\phi_{n,i}\rangle, \qquad (23)$$

and make the tight-binding-like ansatz

$$|\psi_{\mathbf{k},\zeta}\rangle = \sum_{i=1}^{\nu_{\max}+1} \gamma_{\zeta,i}\ |\phi_{\mathbf{k},i}\rangle, \qquad (24)$$

with the variational parameters $\gamma_{\zeta,i}$ for a propagating magnetic polaron. This leads to a Hermitian eigenvalue problem with the $(\nu_{\max}+1)\times(\nu_{\max}+1)$ Hamilton matrix

$$H^{(b)}_{\mathbf{k}} = \mathbf{E} + \frac{\epsilon_{\mathbf{k}}}{2}\ \mathbf{B}, \qquad (25)$$

where $\mathbf{E} = \mathrm{diag}(E_1, E_2, \ldots, E_{\nu_{\max}+1})$, $B_{i,j} = \beta_{0,i}\beta_{0,j}$, and $\epsilon_{\mathbf{k}} = -2t[\cos(k_x) + \cos(k_y)]$. Figure 1 shows the resulting energy bands $E_{\mathbf{k}}$ for the propagating polaron where the different bands originate from the individual *string levels* E_i. The figure illustrates the convergence of the low energy bands with increasing cutoff $\nu_{\max}$ for the length of the string. Figure 2 compares the *bare* single-fermion dispersion $3J/4 + \epsilon_{\mathbf{k}}/2$ to the variational result for the lowest band, $\zeta = 1$, for different J. All bands are shifted such that the band bottom at $\mathbf{k} = (0,0)$ has energy zero. While the bands for different J have similar curvature around $\mathbf{k} = (0,0)$, the curvature varies strongly with J around $\mathbf{k} = (\pi,\pi)$. Put another way, the quite substantial band narrowing for small J occurs predominantly around the band maximum at $\mathbf{k} = (\pi,\pi)$. The mechanism which leads to this band narrowing becomes apparent in Fig. 3, which shows the $\mathbf{k}$ dependence of the magnetic polaron wave function for the lowest band:

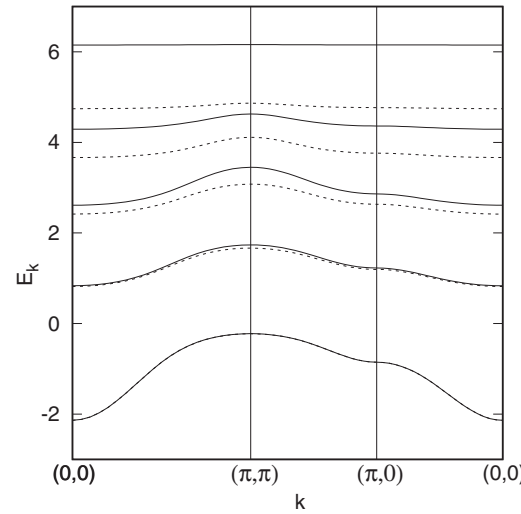

FIG. 1. Band dispersion $E_{\mathbf{k}}$ (in units of t) for a single $b^\dagger$ fermion, $J = 1$. The figure compares results for $\nu_{\max} = 4$ (full line) and $\nu_{\max} = 8$ (dotted line).

$$\beta_{\nu,\mathrm{tot}}(\mathbf{k}) = \sum_i \gamma_{\zeta,1}(\mathbf{k})\ \beta_{\nu,i}. \qquad (26)$$

As $\mathbf{k}$ moves from $(0,0) \to (\pi,\pi)$ the wave function $\beta_{\nu,\mathrm{tot}}$ expands, i.e., the amplitude for $\nu = 0$ becomes small and the weight of longer strings increases. This is what one would expect intuitively because for $\mathbf{k} \to (\pi,\pi)$ it becomes more and more unfavorable for the fermion to propagate because $\epsilon_{\mathbf{k}}$ becomes large and positive. The magnetic polaron wave function $\beta_{\nu,\mathrm{tot}}$ reacts to this by expanding so that its amplitude at the center, $\beta_{0,\mathrm{tot}}$, becomes smaller and the expectation value of coherent intersite hopping, which is $\beta^2_{0,\mathrm{tot}}\ \epsilon_{\mathbf{k}}/2$, becomes less positive, whereas for $\mathbf{k} \to (0,0)$ the magnetic polaron

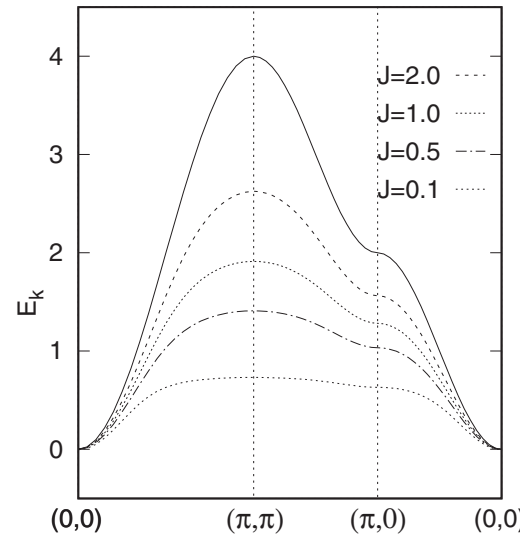

FIG. 2. Dispersion $E_{\mathbf{k}}$ (in units of t) for a single $b^\dagger$ fermion for different J (dashed lines) compared to the unrenormalized band structure $\frac{3J}{4} + \frac{\epsilon_{\mathbf{k}}}{2}$ (full line). A J-dependent constant has been subtracted from all bands to align them at $\mathbf{k} = (0,0)$.

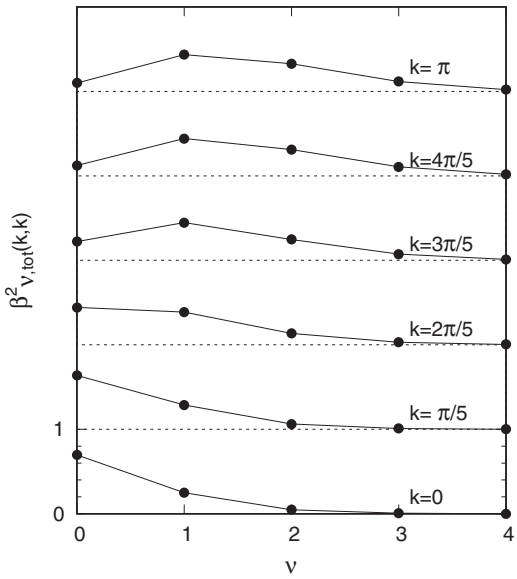

FIG. 3. Magnetic polaron wave function $\beta^2_{\nu,\mathrm{tot}}(k,k)$ for the lowest band for different k, $J = 0.5$.

contracts so as to maximize the energy gain due to polaron propagation, $\beta^2_{0,\mathrm{tot}}\,\epsilon_{\mathbf{k}}/2$. Figure 3 refers to $J = 0.5$; it is obvious that as J becomes smaller the cost in energy for expanding the polaron—and hence to minimize $\beta^2_{0,\mathrm{tot}}$—becomes less and less. For this reason, we expect that in the heavy part of the band the magnetic polaron is more extended, i.e., the number of triplets carried by the fermion is larger than for the strongly dispersive part near $\mathbf{k} = (0, 0)$. This is also confirmed by Fig. 4, which shows the number of triplets $n_t = \sum_n \langle \boldsymbol{t}^\dagger_n \cdot \boldsymbol{t}_n \rangle$ in the polaron state for the lowest band as a function of $\mathbf{k}$ for various J. For momenta near (π, π) and small J this is large, which shows that the polaron becomes extended in real space.

Had we started from a state with a single $a^\dagger$ fermion at site n_0 instead of (10) we would have obtained the same equations but throughout $\tilde{t} \to -\tilde{t}$ and $\epsilon_{\mathbf{k}} \to -\epsilon_{\mathbf{k}}$ because the

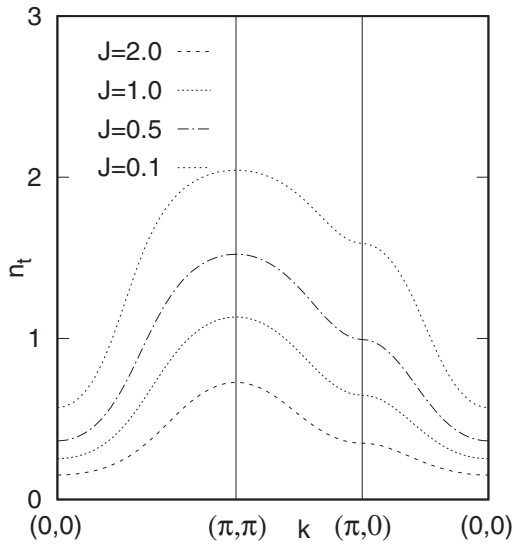

FIG. 4. *Triplet content* n_t for the lowest magnetic polaron state of a single $b^\dagger$ fermion as a function of wave vector $\mathbf{k}$.

hopping integral for a holelike fermion has opposite sign as compared to the electronlike fermion. If we choose the same $\nu_{\max}$ for the $a^\dagger$-like polaron—which we do in all that follows—the energies E_i are the same and the polaron wave functions can be obtained by a gauge transformation: $\beta_{\nu,i} \to (-1)^\nu\ \beta_{\nu,i}$.

To conclude this section we discuss the representation of the operator N_{ft} which counts the total number of fermions and triplets:

$$N_{ft} = \sum_n \left[\sum_\sigma (a^\dagger_{n,\sigma} a_{n,\sigma} + b^\dagger_{n,\sigma} b_{n,\sigma}) + \boldsymbol{t}^\dagger_n \cdot \boldsymbol{t}_n \right]. \quad (27)$$

Each string state $|n_0, n_1, n_2, \ldots, n_\nu\rangle$ is an eigenstate of N_{ft} with eigenvalue $\nu + 1$, from which we obtain

$$\langle \phi_{m,i} | N_{ft} | \phi_{n,j} \rangle = \delta_{m,n} \sum_{\nu=0}^{\infty} (\nu + 1) \beta_{\nu,i}\ \beta_{\nu,j} = \delta_{m,n}\, \tilde{n}_{i,j}. \quad (28)$$

IV. FULL HAMILTONIAN

So far we have studied a single fermion and found that it creates a $\mathbf{k}$-dependent dressing cloud of triplets around itself. The discussion is incomplete, however, because we have neglected the fact that there are pair creation processes—described by the second term in H_1 in (7)—where pairs of $a^\dagger$ fermions and $b^\dagger$ fermions are created/annihilated, so there never will be a single $b^\dagger$ fermion in the lattice. It seems reasonable to assume, however, that all $a^\dagger$ fermions and $b^\dagger$ fermions also will surround themselves by a triplet cloud with $\mathbf{k}$-dependent structure so as to optimize the energy. Before we proceed with this problem, however, we need to consider the *hard core constraint* (3) inherent in the bond particle formalism. In the calculations so far this has been taken into account exactly, because all string states such as (10) and (11) do obey this constraint exactly. For the case of a system with a finite density of fermions and triplets, however, we are forced to make approximations. One possibility is the Gutzwiller approximation [77] but here we follow the simpler treatment of Jurecka and Brenig [63]. These authors assumed that the singlet bosons created by $s^\dagger_n$ can be taken as condensed and thus the singlet creation and annihilation operators can be replaced by a real condensation amplitude s which moreover is taken as site independent:

$$s^\dagger_m \to s, \quad s_m \to s. \quad (29)$$

The constraint (3) then becomes

$$N(1 - s^2) - N_{f,t} = 0 \quad (30)$$

and the relevant part of the Hamiltonian changes to

$$H_1 = \sum_n \left(\frac{3J}{4} \sum_\sigma (b^\dagger_{n,\sigma} b_{n,\sigma} + a^\dagger_{n,\sigma} a_{n,\sigma}) + J\, \boldsymbol{t}^\dagger_n \cdot \boldsymbol{t}_n \right)$$
$$+ \sum_{m,n} \frac{s^2\, t_{m,n}}{2} \left\{ \sum_\sigma (b^\dagger_{m,\sigma} b_{n,\sigma} - a^\dagger_{m,\sigma} a_{n,\sigma}) \right.$$

$$-[(b^\dagger_{m,\uparrow}a^\dagger_{n,\downarrow} - b^\dagger_{m,\downarrow}a^\dagger_{n,\uparrow}) + \text{H.c.}]\Big\}$$
$$- \sum_{m,n} \frac{s\, t_{m,n}}{2}\, (\boldsymbol{b}_{m,n} - \boldsymbol{a}_{m,n}) \cdot (\boldsymbol{t}^\dagger_n + \boldsymbol{t}_m). \tag{31}$$

Without the pair creation terms $\propto b^\dagger_{m,\uparrow}a^\dagger_{n,\downarrow} - b^\dagger_{m,\downarrow}a^\dagger_{n,\uparrow}$ this would be the combination of two decoupled Hamiltonians describing the propagation of the $b^\dagger$ fermions and the $a^\dagger$ fermions which we have treated in the preceding section, the only difference being that the hopping integrals are renormalized by the factors of s^2 and s. It is the pair creation term which couples these problems and establishes an equilibrium concentration of fermions. To get an idea how this problem can be treated we note that the eigenvalue problem (25) may be thought of as having been obtained from the effective Hamiltonian:

$$H_{\text{eff}} = \sum_{\mathbf{k},\sigma} \Bigg(\sum_{i,j=1}^{\nu_{\max}+1} H^{(b)}_{\mathbf{k},i,j}\, \tilde{b}^\dagger_{\mathbf{k},i,\sigma} \tilde{b}_{\mathbf{k},j,\sigma} + \sum_{i,j=1}^{\nu_{\max}+1} H^{(a)}_{\mathbf{k},i,j}\, \tilde{a}^\dagger_{\mathbf{k},i,\sigma} \tilde{a}_{\mathbf{k},j,\sigma} \Bigg), \tag{32}$$

where $H^{(a)}_{\mathbf{k}}$ is obtained from $H^{(b)}_{\mathbf{k}}$ by replacing $\epsilon_{\mathbf{k}} \to -\epsilon_{\mathbf{k}}$. In this effective Hamiltonian each of the localized polaron states $|\phi_{n,i}\rangle$ is considered as an *effective fermion*, created by $\tilde{b}^\dagger_{n,i,\sigma}$ and similar for the holelike polarons.

Next, the pair creation term $b^\dagger_{m,\uparrow}a^\dagger_{n,\downarrow}$ creates a $b^\dagger$ fermion and an $a^\dagger$ fermion at sites m and n, which would have the coefficients $\beta_{0,i}$ and $\beta_{0,j}$ in their respective polaron states described by $\tilde{b}^\dagger_{m,i,\sigma}\tilde{a}^\dagger_{n,j,\bar{\sigma}}$. Therefore, to incorporate the pair-creation process consistently we augment the Hamiltonian (32) by

$$H'_{\text{eff}} = \sum_{\mathbf{k},\sigma} \sum_{i,j=1}^{\nu_{\max}+1} \Delta_{\mathbf{k},i,j,\sigma}\, \tilde{b}^\dagger_{\mathbf{k},i,\sigma} \tilde{a}^\dagger_{-\mathbf{k},j,\bar{\sigma}} + \text{H.c.}, \tag{33}$$
$$\Delta_{\mathbf{k},i,j,\sigma} = -\frac{\epsilon_{\mathbf{k}}}{2}\, \beta_{0,i}\, \beta_{0,j}\, \text{sign}(\sigma). \tag{34}$$

Note that we are actually making a simplification here: if a $\tilde{b}^\dagger$ fermion and an $\tilde{a}^\dagger$ fermion are pair created on nearest neighbors, the respective polaron wave functions $\beta_{i,\nu}$ would have to be modified because for each of the fermions the number of neighbors available for the first hop is $z-1$ rather than z. The matrix element for hopping of the magnetic polaron away from the site where it was created therefore would be slightly different than that for hopping *in empty space*. This would result in an effective interaction between $\tilde{b}^\dagger$ fermions and $\tilde{a}^\dagger$ fermions. The same would actually happen if any two of these polarons come close to each other and their triplet clouds overlap. However, we neglect this interaction in the following. Lastly, the operator $N_{f,t}$ which counts fermions and triplets becomes

$$N_{f,t} = \sum_{\mathbf{k},\sigma} \sum_{i,j=1}^{\nu_{\max}+1} \tilde{n}_{i,j}\, (\tilde{b}^\dagger_{\mathbf{k},i,\sigma}\tilde{b}_{\mathbf{k},j,\sigma} + \tilde{a}^\dagger_{\mathbf{k},i,\sigma}\tilde{a}_{\mathbf{k},j,\sigma}) \tag{35}$$

with $\tilde{n}_{i,j}$ given in (28). Using this the constraint (30) can be added to the Hamiltonian with Lagrange multiplier λ.

The resulting Hamiltonian is readily diagonalized by canonical transformation, i.e., we make the ansatz

$$\gamma^\dagger_{\mathbf{k},\zeta,\sigma} = \sum_i (u_{\mathbf{k},\zeta,i}\, \tilde{b}^\dagger_{\mathbf{k},i,\sigma} + v_{\mathbf{k},\zeta,i}\, \tilde{a}_{-\mathbf{k},i,\bar{\sigma}}) \tag{36}$$

and demand $[H^{\text{tot}}_{\text{eff}}, \gamma_{\mathbf{k},\zeta,\sigma}] = E_{\mathbf{k}}\gamma_{\mathbf{k},\zeta,\sigma}$. This results in a Hermitian eigenvalue problem the dimension of which now is $(2\nu_{\max}+2)\times(2\nu_{\max}+2)$:

$$H = \begin{pmatrix} \mathbf{E} + \frac{\epsilon_{\mathbf{k}}}{2}\,\mathbf{B} - \lambda\tilde{n} & -\frac{\epsilon_{\mathbf{k}}}{2}\,\mathbf{B}\ \text{sign}(\sigma) \\ -\frac{\epsilon_{\mathbf{k}}}{2}\,\mathbf{B}^+\ \text{sign}(\sigma) & -\mathbf{E} + \frac{\epsilon_{\mathbf{k}}}{2}\,\mathbf{B}^* + \lambda\tilde{n} \end{pmatrix}. \tag{37}$$

The *central bands*, i.e., $\zeta = \nu_{\max}+1$ and $\nu_{\max}+2$, again converge rapidly with the cutoff $\nu_{\max}$.

Let us next consider the electron number, more precisely the sum of both c electrons and f electrons:

$$N_e = \sum_{i,\sigma} (f^\dagger_{i,\sigma} f_{i,\sigma} + c^\dagger_{i,\sigma} c_{i,\sigma}). \tag{38}$$

The *vacuum state* has a singlet at each site and therefore $2N$ electrons. Each $\tilde{a}^\dagger$ quasiparticle corresponds to a superposition of states with precisely one $a^\dagger$ fermion and a variable number of triplets. Since the triplets have the same number of electrons as the singlets—namely two—the $\tilde{a}^\dagger$ quasiparticle reduces N_e by one. Similarly, a $\tilde{b}^\dagger$ quasiparticle increases N_e by one and we find

$$\begin{aligned} N_e &= 2N + \sum_{\mathbf{k},\sigma} \sum_{\nu=0}^{\nu_{\max}} (b^\dagger_{\mathbf{k},\nu,\sigma} b_{\mathbf{k},\nu,\sigma} - a^\dagger_{\mathbf{k},\nu,\sigma} a_{\mathbf{k},\nu,\sigma}) \\ &= \sum_{\mathbf{k},\sigma} \sum_{\nu=0}^{\nu_{\max}} (b^\dagger_{\mathbf{k},\nu,\sigma} b_{\mathbf{k},\nu,\sigma} + a_{\mathbf{k},\nu,\sigma} a^\dagger_{\mathbf{k},\nu,\sigma}) - 2N\nu_{\max} \\ &= \sum_{\mathbf{k},\sigma} \sum_{\zeta=1}^{2\nu_{mx}+2} \gamma^\dagger_{\mathbf{k},\zeta,\sigma}\gamma_{\mathbf{k},\zeta,\sigma} - 2N\nu_{\max}. \end{aligned} \tag{39}$$

The first term on the right-hand side is the total number of quasiparticles. If we assume for simplicity that the quasiparticle bands do not overlap, the lowest $\nu_{\max}$ bands must be filled completely, whereas the central bands $\zeta = \nu_{\max}+1$ and $\nu_{\max}+2$ must be filled such that the number of occupied $\mathbf{k}$ points corresponds to the the number of *both* $c^\dagger$ electrons *and* $f^\dagger$ electrons, i.e., the Luttinger theorem is fulfilled. This is actually true already for the simplest form of bond particle theory [66]—which is obtained by setting $\nu_{\max} = 0$ in all the above calculations—and this highly desirable property also transfers to the magnetic polaron Hamiltonian.

As already mentioned we restrict ourselves to the case $N_e = 2N$ so that the Fermi energy coincides with the center of the gap between the two central bands. The parameters s^2 and λ then have to be determined by minimization of the ground

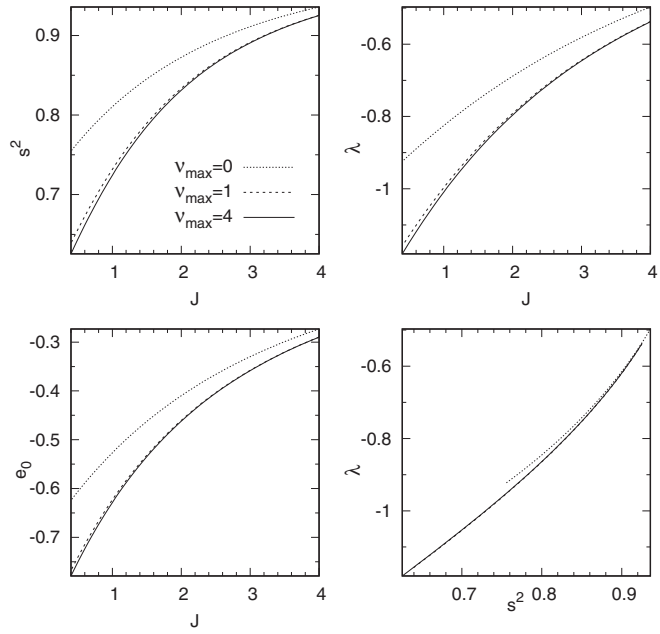

FIG. 5. The values of s^2, λ, and the ground state energy per site, e_0, vs J for different $\nu_{\max}$.

state energy per site:

$$e_0 = \frac{2}{N}\sum_{\mathbf{k}}\sum_{\lambda=1}^{\nu_{\max}+1} E_{\lambda,\mathbf{k}} - \lambda(s^2 - 1 + 2\ \mathrm{tr}\ \tilde{n}) + 2\mathrm{tr}\ \mathbf{E} \tag{40}$$

where we used $\sum_{\mathbf{k}} \epsilon_{\mathbf{k}} = 0$. Figure 5 shows s^2, λ, and e_0 as functions of J, calculated with different string length $\nu_{\max}$. In particular $\nu_{\max} = 0$ is equivalent to the original theory of Jurecka and Brenig [63], where no strings are taken into account. Already $\nu_{\max} = 1$ gives quite a substantial lowering of the ground state energy e_0 and the results then converge rapidly with $\nu_{\max}$. For small J the value of s^2 is reduced as compared to $\nu_{\max} = 0$, which is clear because with $\nu_{\max} > 0$ also the triplet cloud contributes to $N_{f,t}$. This is also the reason why the parameter λ is more negative than for $\nu_{\max} = 0$. Adding the constraint to the Hamiltonian means replacing the energy of the triplet from $J \to J - \lambda$ and that of the fermions from $3J/4 \to 3J/4 - \lambda$.

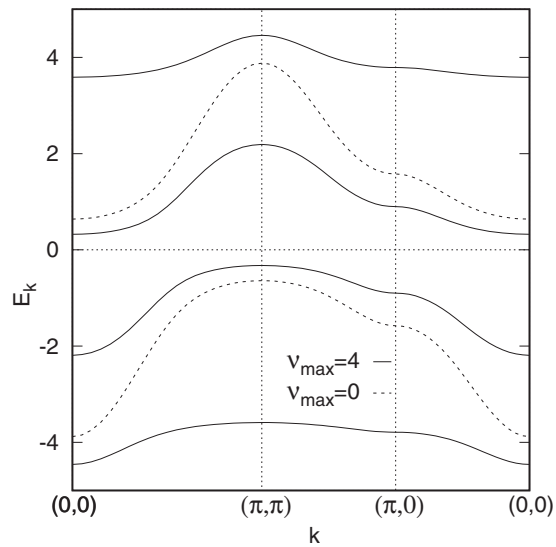

FIG. 6. Band structure for $J = 1$ for $\nu_{\max} = 0$ and 4. For $\nu_{\max} = 4$ only four of the ten bands are shown.

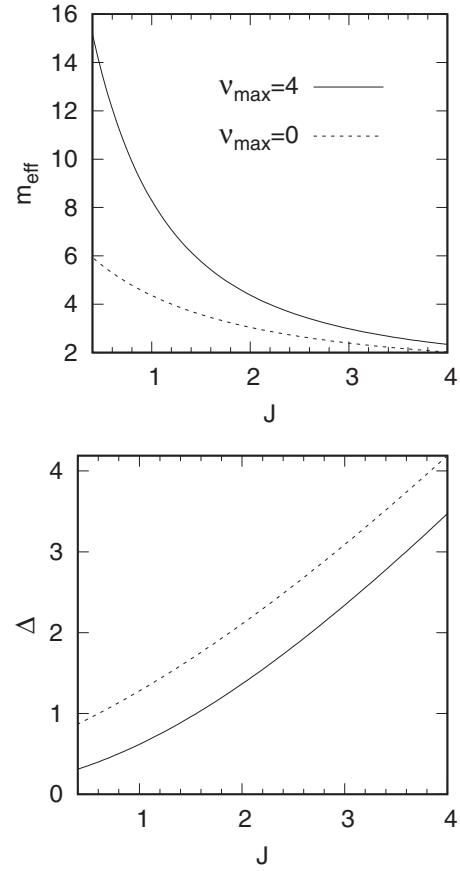

FIG. 7. Effective mass m_{eff} for the heavy part of the band structure at (π, π) and quasiparticle gap Δ between $\mathbf{k} = (0, 0)$ and (π, π) vs J for $\nu_{\max} = 0$ and 4.

Figure 6 shows the band structure for $J = 1$ and $\nu_{\max} = 0$ and 4, both calculated with the respective self-consistent

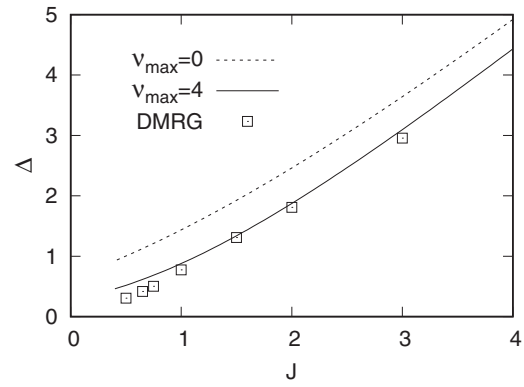

FIG. 8. Quasiparticle gap Δ between $k = 0$ and π vs J for $\nu_{\max} = 0$ and 4 for the one-dimensional KLM compared to DMRG results by Yu and White [29] (DMRG).

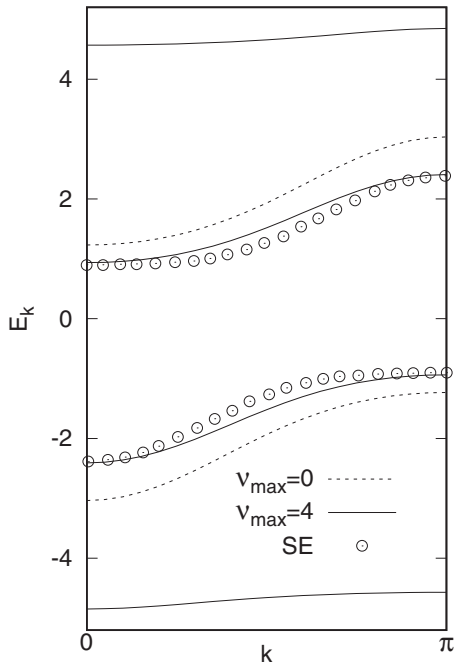

FIG. 9. Band structure at $J = 2$ for the one-dimensional KLM from the present theory compared to the series expansion result by Trebst *et al.* [42] (SE).

parameters. For $\nu_{\max} > 0$ additional sidebands appear roughly at the energies of the string levels. Together with the smaller values of s^2 this leads to a reduction of the bandwidth of the central bands. Figure 7 shows the effective mass $m_{\text{eff}} = (\frac{\partial^2 E_{\mathbf{k}}}{\partial k_x^2})^{-1}$ of the lower central band, $\nu_{\max} + 1$, at $\mathbf{k} = (\pi, \pi)$ and the energy gap between the two central bands versus J. For $J \leqslant 1$ polaron formation results in an appreciable enhancement of the effective mass, and at the same time the gap is reduced substantially.

To conclude this section we apply the present theory to the one-dimensional KLM and compare with numerical results. Figure 8 compares the quasiparticle gap Δ for the one-dimensional model to the numerical results of Yu and White [29] obtained by density matrix renormalization group (DMRG) calculation. Inclusion of the magnetic polaron effect obviously improves the agreement with numerics significantly. This can also be seen in Fig. 9, which shows the band structure for the one-dimensional model at $J = 2$ and the bands obtained by Trebst *et al.* [42] via series expansion. The magnetic polaron effect significantly improves the agreement with respect to bandwidth and quasiparticle gap, although the mass enhancement near $k = \pi$ obviously is still not sufficient to obtain good agreement with numerics.

V. SUMMARY AND DISCUSSION

In summary, we have investigated a mechanism for enhanced band mass in the KLM, namely the formation of magnetic polarons. This mechanism is quite well known from the problem of hole motion in an antiferromagnet [68–72] and the present theory largely adapts these ideas to the KLM. The essence can be seen already by considering the motion of a single hole in the half-filled KLM: the hole can on one hand gain kinetic energy by creating and reabsorbing strings of triplets, and on the other hand it can avoid coherent motion in those parts of the Brillouin zone where free propagation would increase the energy, i.e., where $\epsilon_{\mathbf{k}} > 0$. This also implies that the spatial extent of the polaron wave function depends on its wave vector $\mathbf{k}$: the polaron contracts when coherent propagation lowers the energy and expands in the opposite case. We have also investigated the full Kondo lattice, but while in the case of the single-hole problem the constraint inherent in the bond particle formulation of the KLM could be taken into account rigorously, for the full Kondo lattice we had to resort to the mean-field procedure of Jurecka and Brenig [63] to deal with this constraint. This is somewhat unsatisfactory because it is ultimately an uncontrolled approximation, but the results indicate that the magnetic polaron effect yields an enhancement of the mass in the heavy parts of the quasiparticle bands also in the framework of this formalism. While for the extreme Kondo limit $J/t \ll 1$ the results of the mean-field procedure probably have at best qualitative significance, they are probably reasonably reliable for $J/t \geqslant 1$—this is also suggested by the agreement with numerics demonstrated in Figs. 8 and 9. At this point it may be worth noting that using the mean-field approximation Jurecka and Brenig obtained the critical value $J/t = 1.5$ for antiferromagnetic ordering in the half-filled Kondo lattice [63] in very good agreement with the exact value of $J/t = 1.45 \pm 0.05$ found by quantum Monte Carlo [39].

As a second major approximation we have neglected a number of terms in the Hamiltonian (7), i.e., the parts H_2 and H_4. These terms are quadratic in both the fermion operators and the triplet operators and thus could be treated in mean-field approximation. For the case of H_2 this has actually been carried out in Ref. [65] and it was found that the resulting correction to the dispersion was relatively small. The terms H_4 would produce exotic magnetic order parameters such as $\langle \boldsymbol{t}_n^\dagger \times \boldsymbol{t}_m \rangle$ or $\langle \boldsymbol{t}_n^\dagger \times \boldsymbol{t}_m^\dagger \rangle$ in a mean-field description, and it is plausible that these are zero in a nonmagnetic phase. When H_2 and H_4 are not treated in mean-field approximation they describe scattering between fermions and triplets. Switching to string states instead of the bare fermions, these terms therefore would describe scattering between magnetic polarons and triplets, which in turn would introduce a damping of the resulting quasiparticles as well as some renormalization of the band dispersion. However, for the valence and conduction bands in the Kondo insulator these effects are probably small because they would require scattering across the insulating gap.

Lastly we note that evidence for spin polaron formation can also be seen in exact diagonalization calculations for the PAM [48], in that the single particle spectral function of *diagnostic operators* which describe an electron accompanied by a spin excitation shows enhanced spectral weight for the heavy bands. All in all it therefore seems plausible that the formation of magnetic polarons may play a role in the enormous mass enhancement observed in heavy fermion materials.

[1] G. R. Stewart, Heavy-fermion systems, Rev. Mod. Phys. **56**, 755 (1984).

[2] P. A. Lee, T. M. Rice, J. W. Serene, L. J. Sham, and J. W. Wilkins, Theories of heavy-electron systems, Comm. Condens. Matter Phys. **12**, 99 (1986).

[3] J. R. Schrieffer and P. A. Wolff, Relation between the Anderson and Kondo Hamiltonians, Phys. Rev. **149**, 491 (1966).

[4] K. Yosida, Bound state due to the s-d exchange interaction, Phys. Rev. **147**, 223 (1966).

[5] C. M. Varma and Y. Yafet, Magnetic susceptibility of mixed-valence rare-earth compounds, Phys. Rev. B **13**, 2950 (1976).

[6] O. Gunnarsson and K. Schönhammer, Electron spectroscopies for Ce compounds in the impurity model, Phys. Rev. B **28**, 4315 (1983).

[7] A. Yoshimori and A. Sakurai, Functional integral approach to the bound state due to the s-d exchange interaction, Prog. Theor. Phys. Suppl. **46**, 162 (1970).

[8] N. Read and D. M. Newns, On the solution of the Coqblin-Schrieffer Hamiltonian by the large-N expansion technique, J. Phys. C **16**, 3273 (1983).

[9] H. Keiter and J. C. Kimball, Diagrammatic perturbation technique for the Anderson Hamiltonian, and relation to the s-d exchange Hamiltonian, Int. J. Magn. **1**, 233 (1971).

[10] Y. Kuramoto, Self-consistent perturbation theory for dynamics of valence fluctuations, Z. Phys. B **53**, 37 (1983).

[11] P. Coleman, New approach to the mixed-valence problem, Phys. Rev. B **29**, 3035 (1984).

[12] N. E. Bickers, Review of techniques in the large-N expansion for dilute magnetic alloys, Rev. Mod. Phys. **59**, 845 (1987).

[13] K. G. Wilson, The renormalization group: Critical phenomena and the Kondo problem, Rev. Mod. Phys. **47**, 773 (1975).

[14] N. Andrei, K. Furaya, and J. H. Lowenstein, Solution of the Kondo problem, Rev. Mod. Phys. **55**, 331 (1983).

[15] C. Lacroix and M. Cyrot, Phase diagram of the Kondo lattice, Phys. Rev. B **20**, 1969 (1979).

[16] C. Lacroix, Some exact results for the Kondo lattice with infinite exchange interaction, Solid State Commun. **54**, 991 (1985).

[17] A. Auerbach and K. Levin, Kondo bosons and the Kondo lattice: Microscopic basis for the heavy Fermi liquid, Phys. Rev. Lett. **57**, 877 (1986).

[18] S. Burdin, A. Georges, and D. R. Grempel, Coherence scale of the Kondo lattice, Phys. Rev. Lett. **85**, 1048 (2000).

[19] G.-M. Zhang and L. Yu, Kondo singlet state coexisting with antiferromagnetic long-range order: A possible ground state for Kondo insulators, Phys. Rev. B **62**, 76 (2000).

[20] M. Lavagna and C. Pepin, Critical phenomena near the antiferromagnetic quantum critical point of heavy fermions, Phys. Rev. B **62**, 6450 (2000).

[21] T. Senthil, M. Vojta, and S. Sachdev, Weak magnetism and non-Fermi liquids near heavy-fermion critical points, Phys. Rev. B **69**, 035111 (2004).

[22] M. Vojta, From itinerant to local-moment antiferromagnetism in Kondo lattices: Adiabatic continuity versus quantum phase transitions, Phys. Rev. B **78**, 125109 (2008).

[23] G.-M. Zhang, Y.-H. Su, and L. Yu, Lifshitz transitions in a heavy Fermi liquid driven by short-range antiferromagnetic correlations in the two-dimensional Kondo lattice model, Phys. Rev. B **83**, 033102 (2011).

[24] J. Nilsson, Fermionic representations of the Kondo lattice model, Phys. Rev. B **83**, 235103 (2011).

[25] X. Montiel, S. Burdin, C. Pepin, and A. Ferraz, Modulated spin-liquid and magnetic order from a Kondo-Heisenberg model applied to URu_2Si_2, Phys. Rev. B **90**, 045125 (2014).

[26] S. Viola Kusminskiy, K. S. D. Beach, A. H. Castro Neto, and D. K. Campbell, Mean-field study of the heavy-fermion metamagnetic transition, Phys. Rev. B **77**, 094419 (2008).

[27] A. J. Millis and P. A. Lee, Large-orbital-degeneracy expansion for the lattice Anderson model, Phys. Rev. B **35**, 3394 (1987).

[28] D. M. Newns and N. Read, Mean-field theory of intermediate valence/heavy fermion systems, Adv. Phys. **36**, 799 (1987).

[29] C. C. Yu and S. R. White, Numerical renormalization group study of the one-dimensional Kondo insulator, Phys. Rev. Lett. **71**, 3866 (1993). The DMRG data for the ground state energy are not published in this reference but seem to be given only in Ref. [40].

[30] S. Moukouri and L. G. Caron, Ground-state properties of the one-dimensional Kondo lattice at partial band filling, Phys. Rev. B **52**, R15723(R) (1995).

[31] S. Moukouri and L. G. Caron, Fermi surface of the one-dimensional Kondo-lattice model, Phys. Rev. B **54**, 12212 (1996).

[32] T. Mutou, N. Shibata, and K. Ueda, Temperature-induced gap formation in dynamic correlation functions of the one-dimensional Kondo insulator: Finite-temperature density-matrix renormalization-group study, Phys. Rev. Lett. **81**, 4939 (1998).

[33] S. Smerat, U. Schollwöck, I. P. McCulloch, and H. Schoeller, Quasiparticles in the Kondo lattice model at partial fillings of the conduction band using the density matrix renormalization group, Phys. Rev. B **79**, 235107 (2009).

[34] M. Jarrell, H. Akhlaghpour, and Th. Pruschke, Periodic Anderson model in infinite dimensions, Phys. Rev. Lett. **70**, 1670 (1993).

[35] M. Jarrell, Symmetric periodic Anderson model in infinite dimensions, Phys. Rev. B **51**, 7429 (1995).

[36] A. N. Tahvildar-Zadeh, M. Jarrell, and J. K. Freericks, Low-temperature coherence in the periodic anderson model, Phys. Rev. Lett. **80**, 5168 (1998).

[37] R. Peters and T. Pruschke, Magnetic phases in the correlated Kondo-lattice model, Phys. Rev. B **76**, 245101 (2007).

[38] C. Gröber and R. Eder, Temperature-dependent band structure of the Kondo insulator, Phys. Rev. B **57**, R12659(R) (1998).

[39] F. F. Assaad, Quantum Monte Carlo simulations of the half-filled two-dimensional Kondo lattice model, Phys. Rev. Lett. **83**, 796 (1999).

[40] Z.-P. Shi, R. R. P. Singh, M. P. Gelfand, and Z. Wang, Phase transitions in the symmetric Kondo-lattice model in two and three dimensions, Phys. Rev. B **51**, 15630 (1995).

[41] W. Zheng and J. Oitmaa, Zero-temperature series expansions for the Kondo lattice model at half filling, Phys. Rev. B **67**, 214406 (2003).

[42] S. Trebst, H. Monien, A. Grzesik, and M. Sigrist, Quasiparticle dynamics in the Kondo lattice model at half filling, Phys. Rev. B **73**, 165101 (2006).

[43] H. Watanabe and M. Ogata, Fermi-surface reconstruction without breakdown of Kondo screening at the quantum critical point, Phys. Rev. Lett. **99**, 136401 (2007).

[44] M. Z. Asadzadeh, F. Becca, and M. Fabrizio, Variational Monte Carlo approach to the two-dimensional Kondo lattice model, Phys. Rev. B **87**, 205144 (2013).
[45] K. Kubo, Lifshitz transitions in magnetic phases of the periodic anderson model, J. Phys. Soc. Jpn. **84**, 094702 (2015).
[46] H. Tsunetsugu, Y. Hatsugai, K. Ueda, and M. Sigrist, Spin-liquid ground state of the half-filled Kondo lattice in one dimension, Phys. Rev. B **46**, 3175 (1992).
[47] J. A. White, Numerical exact-diagonalization study of the one-dimensional symmetric Kondo lattice, Phys. Rev. B **46**, 13905 (1992).
[48] K. Tsutsui, Y. Ohta, R. Eder, S. Maekawa, E. Dagotto, and J. Riera, Heavy quasiparticles in the Anderson lattice model, Phys. Rev. Lett. **76**, 279 (1996).
[49] L. C. Martin and F. F. Assaad, Evolution of the Fermi surface across a magnetic order-disorder transition in the two-dimensional Kondo lattice model: A dynamical cluster approach, Phys. Rev. Lett. **101**, 066404 (2008).
[50] L. C. Martin, M. Bercx, and F. F. Assaad, Fermi surface topology of the two-dimensional Kondo lattice model: Dynamical cluster approximation approach, Phys. Rev. B **82**, 245105 (2010).
[51] B. Lenz, R. Gezzi, and S. R. Manmana, Variational cluster approach to superconductivity and magnetism in the Kondo lattice model, Phys. Rev. B **96**, 155119 (2017).
[52] B. Danu, Z. Liu, F. F. Assaad, and M. Raczkowski, Zooming in on heavy Fermions in Kondo lattice models, Phys. Rev. B **104**, 155128 (2021).
[53] M. Oshikawa, Topological approach to Luttinger's theorem and the Fermi surface of a Kondo lattice, Phys. Rev. Lett. **84**, 3370 (2000).
[54] P. Nozières, Some comments on Kondo lattices and the Mott transition, Eur. Phys. J. B **6**, 447 (1998).
[55] S. Sachdev and R. N. Bhatt, Bond-operator representation of quantum spins: Mean-field theory of frustrated quantum Heisenberg antiferromagnets, Phys. Rev. B **41**, 9323 (1990).
[56] S. Gopalan, T. M. Rice, and M. Sigrist, Spin ladders with spin gaps, Phys. Rev. B **49**, 8901 (1994).
[57] M. Vojta and K. W. Becker, Hole dynamics on both sides of a magnetic ordering transition, Phys. Rev. B **60**, 15201 (1999).
[58] S. Ray and M. Vojta, Carrier dynamics in doped bilayer iridates near magnetic quantum criticality, Phys. Rev. B **98**, 115102 (2018).
[59] O. P. Sushkov, Single-hole dynamics in dimerized spin liquids, Phys. Rev. B **60**, 3289 (1999).
[60] K. Park and S. Sachdev, Bond-operator theory of doped antiferromagnets: From Mott insulators with bond-centered charge order to superconductors with nodal fermions, Phys. Rev. B **64**, 184510 (2001).
[61] M. Siahatgar, B. Schmidt, G. Zwicknagl, and P. Thalmeier, Moment screening in the correlated Kondo lattice model, New J. Phys. **14**, 103005 (2012).
[62] R. Eder, O. Stoica, and G. A. Sawatzky, Single-particle excitations of the Kondo lattice, Phys. Rev. B **55**, R6109 (1997); R. Eder, O. Rogojanu, and G. A. Sawatzky, Many-body band structure and Fermi surface of the Kondo lattice, *ibid.* **58**, 7599 (1998).
[63] C. Jurecka and W. Brenig, Bond-operator mean-field theory of the half-filled Kondo lattice model, Phys. Rev. B **64**, 092406 (2001).
[64] V. N. Kotov and P. J. Hirschfeld, The Kondo lattice model from strong-coupling viewpoint, Physica B: Condensed Matter **312-313**, 174 (2002).
[65] R. Eder, Quasiparticle band structure and spin excitation spectrum of the Kondo lattice, Phys. Rev. B **99**, 085134 (2019).
[66] R. Eder, K. Grube, and P. Wróbel, Antiferromagnetic phases of the Kondo lattice, Phys. Rev. B **93**, 165111 (2016).
[67] R. Eder and P. Wróbel, Antiferromagnetic phase of the Kondo insulator, Phys. Rev. B **98**, 245125 (2018).
[68] L. N. Bulaevskii, E. L. Nagaev, and D. L. Khomskii, A New Type of Auto-localized State of a Conduction Electron in an Antiferromagnetic Semiconductor, Sov. Phys. JETP. **27**, 836 (1968).
[69] B. I. Shraiman and E. D. Siggia, Two-particle excitations in antiferromagnetic insulators, Phys. Rev. Lett. **60**, 740 (1988).
[70] S. A. Trugman, Interaction of holes in a Hubbard antiferromagnet and high-temperature superconductivity, Phys. Rev. B **37**, 1597 (1988).
[71] J. Inoue and S. Maekawa, Dynamics of Holes in Antiferromagnetic State, J. Phys. Soc. Jpn. **59**, 2110 (1990).
[72] R. Eder and K. W. Becker, Coherent motion of a hole in a two-dimensional quantum antiferromagnet, Z. Phys. B **78**, 219 (1990).
[73] K. J. vonSzczepanski, P. Horsch, W. Stephan, and M. Ziegler, Single-particle excitations in a quantum antiferromagnet, Phys. Rev. B **41**, 2017 (1990).
[74] E. Dagotto, R. Joynt, A. Moreo, S. Bacci, and E. Gagliano, Strongly correlated electronic systems with one hole, Phys. Rev. B **41**, 9049 (1990).
[75] V. Elser, D. A. Huse, B. I. Shraiman, and E. D. Siggia, Ground state of a mobile vacancy in a quantum antiferromagnet, Phys. Rev. B **41**, 6715 (1990).
[76] B. O. Wells, Z.-X. Shen, A. Matsuura, D. M. King, M. A. Kastner, M. Greven, and R. J. Birgeneau, E versus k relations and many body effects in the model insulating copper oxide $Sr_2CuO_2Cl_2$, Phys. Rev. Lett. **74**, 964 (1995).
[77] M. Keßler and R. Eder, A variational theory of the Kondo lattice, Phys. Rev. B **106**, 045122 (2022).